34th Annual International Conference of the IEEE EMBS
San Diego, California USA, 28 August - 1 September, 2012

A Deformable Cosegmentation Algorithm for Brain MR Images

Tong Zhang, *Student Member, IEEE*, Yong Xia*, *Member, IEEE* and David Dagan Feng, *Fellow, IEEE*

***Abstract*—Cosegmentation aims to simultaneously segment the common parts in a pair of images, and has recently attracted increasing research attention in the field of computer vision. In this paper, we propose a novel deformable cosegmentation (D-C) algorithm to solve the brain MR image segmentation problem by cosegmenting the image and a co-registered atlas. In this manner, the prior heuristic information about brain anatomy that is embedded in the atlas can be transformed into the constraints that control the segmentation of brain MR images. Based on the multiphase Chan-Vese model, the proposed D-C algorithm is implemented using level set techniques. Then, it is compared to the protocol algorithm and the state-of-the-art GA-EM algorithm in T1-weighted brain MR images corrupted by different levels of Gaussian noise and intensity non-uniformity. Our results show that the proposed D-C algorithm can differentiate major brain structures more accuratly and produce more robust segmentation of brain MR images.**

***Index Terms*—Image cosegmentation, Magnetic resonance imaging, deformable model**

I. Introduction

Segmentation of the brain volume into gray matter (GM), white matter (WM), and cerebrospinal fluid (CSF) in magnetic resonance (MR) images plays an essential role in both neuroimaging research and clinical practices. Since the manual segmentation performed by medical professionals is time-consuming, expensive and subject to observer variability, automated brain MR image segmentation has been studied extensively. A number of segmentation algorithms have been proposed in the literature, which can be roughly classified into (a) atlas-based [1-3], (b) statistical [4-6] and (c) deformable model based [7-9].

The basic idea of atlas-based segmentation algorithms is to generate an "average" brain structure representation, i.e. an atlas, from the training image set or anatomy, and then to map the anatomical structure from the atlas to the to-be-segmented image through co-registration [2]. However, the performance of these algorithms is limited by the anatomical variation across individuals and the accuracy of atlas generation and registration. In statistical segmentation algorithms, brain voxel values are generally assumed to follow a statistical model, whose parameters can be estimated according to certain criteria, such as the maximum likelihood principle. Based on the estimated model parameters, voxels can be classified into a particular brain tissue type by using the Bayes classifier. Despite their prevalence, these algorithms face the difficulty of incorporating the anatomical information into the segmentation process. Geometric deformable model based algorithms convert the problem of segmenting an image into that of evolving a boundary curve through minimizing the associated energy function. Due to the complexity of curve evolution, level set theory based techniques are often used to solve this optimization problem. A typical example is the Mumford-Shah segmentation algorithm [7], which assumes that the best decomposition of an image is its optimal piecewise smooth approximations and uses the level set method for the curve approximation. As a modification to this algorithm, the Chan-Vese model [8] incorporates the edge function into the classical active counter algorithm to effectively and robustly segment noisy images without smooth boundaries. Vese and Chan [9] has further extended the two-phase level set model to a multiphase model for multiclass segmentation problems.

Recently, the idea of "cosegmentation" has attracted increasing research attention, which aims to simultaneously segment the common parts in a pair of images by taking the advantages of processing each image with the additional constraint derived from the other image. The cosegmentation task can be formulated as an optimization problem that minimizes the combination of two energy terms [10-12]. The data modality term is usually defined as the normalized difference between the histograms of both images, whereas the spatial regularization term is often derived based on the Markov random field (MRF) model. Meng et al. [13] futher researched on sloving the co-segmentation problem via active counters.

When the prior anatomical information is interpreted by a brain atlas, it is intuitive to apply cosegmentation techniques to the segmentation of brain images, i.e. simultaneously delineating major brain structures in a test image and a reference image generated by using both its statistical information and the co-registered atlas. In this way, the prior anatomical information embedded in the atlas can be used as constraints in the segmentation process. Motivated by this idea, we propose a novel deformable cosegmentation (D-C) algorithm for delineating GM, WM and CSF in brain MR images. Specifically, we modified the multiphase Chan-Vese model by including both the statistical and shape information of the image pairs into the energy function. Then, we compared the proposed D-C algorithm to the protocol algorithm [9] and the state-of-art GA-EM algorithm [6] in T1-weighted brain MR images from BrainWeb [14].

II. Method

A. Related Works

Let us first recall the Mumford and Shah model and Chan-Vese model. Let $I: \Omega \rightarrow R$ be the observed image

Manuscript received April 1 2012. This research is supported by ARC grants.

T. Zhang, Y. Xia, and D. Feng are with the Biomedical and Multimedia Information Technology (BMIT) Research Group, School of Information Technologies, University of Sydney, Sydney, NSW 2006, Australia (e-mail: {tong, yxia, feng}@it.usyd.edu.au).

D. Feng is also with the Med-X Research Institute, Shanghai JiaoTong University, Shanghai 200025, China.

function. A curve C is defined as a closed subset in Ω, which consists of two regions: the foreground Ω_1 and background Ω_2. The Mumford and Shah model aims to segmentation the image into foreground and background by evolving the curve C through minimize the following objective function [7]

$$F_{M-S}(L,C) = \int_{\Omega} [L(x,y) - I(x,y)]^2 dxdy + \mu \int_{\Omega \setminus C} |\nabla L|^2 dxdy + v|C| \quad (1)$$

where L is the optimal piecewise smooth approximation of the initial image I, and $|C|$ denote the length of the curve C and serves as a regularization term.

Chan and Vese [8] proposed a level set based representation of Eq. (1) by assuming the segmented image L to be piecewise constant functions, i.e. if $(x,y) \in \Omega_1$, $L(x,y) \equiv c_1$; otherwise $L(x,y) \equiv c_2$. Thus, the objective energy function in the Chan-Vese model can be written as

$$E_{C-V}(c_1,c_2,C) = \int_{\Omega_1} [I(x,y) - c_1]^2 dxdy + \int_{\Omega_2} [I(x,y) - c_2]^2 dxdy + v|C| \quad (2)$$

Vese and Chan [9] have further extended their research and proposed the multiphase Chan-Vese model for multi-class image segmentation. In this moedel, an image I can be devided into n regions by evolving a collection of counters $C = (C_1, C_2, \cdots, C_m)$ via minimizing the following energy

$$E_{multi}(c,C) = \sum_{j=1}^{n} \int_{\Omega_j} \left[I(x,y) - c_j\right]^2 dxdy + v \sum_{i=1}^{m} |C_i| \quad (3)$$

where $m = \log_2 n$, c_j is the mean voxel value in the region Ω_j, and $c = (c_1, c_2, \cdots, c_n)$.

B. D-C Model

Cosegmentation algorithms aim to simutously segment similar target regions in a pair of images. For brain image cosegmentation, we need a prepocessing step to generate a reference image for each test brain image.

To use the prior anatomical information embedded in the brain atlas, we construct a reference image for each brain image using the co-registered atlas and its own statistical features. We assume that the overlapped region between the hard segmentation results gained by the atlas and the statistical method is the stable segmented area. Specifically, we use the K-means method to acquire the initialized segmentation results with the mean value of each class. At the same time, the atlas of each tissue is normalized and set the voxel values over 0.5 as a hard segmentation for each class. Therefore, the reference image is generated by setting its voxel values in the stable segmented area to the corespanding mean value and that of the other regions the same as the original ones.

Let the image pair of the test image and the constructed reference image be denoted by $I = \{I_0, I_1\}$. We use the evolving counters $C = (C_0, C_1)$ to delineate GM, WM and CSF from background in each image. These three regions and the background are denoted by $\Omega_1, \Omega_2, \Omega_3$ and Ω_4, respectively. In the D-C model, the energy function for the kth image is as follows

$$E_{D-C}^{k}(c_{(1-k)}, C_k) = \sum_{j=1}^{4} \int_{\Omega_{kj}} \left[I_k(x,y) - c_{(1-k)j}\right]^2 dxdy + v \sum_{i=1}^{2} |C_{ki}| \quad (4)$$

where Ω_{kj} is the jth region in image I_k, and $c_{(1-k)j}$ is the mean voxel value in jth region in image I_{1-k}. The pair of images can be jointly segmented through minimizing both energy functions, shown as follows

$$C = \min_C \begin{cases} E_{D-C}^{1}(c_0, C_1) \\ E_{D-C}^{0}(c_1, C_0) \end{cases} \quad (5)$$

C. Energy Minimization

Following the formulation of the multiphase Chan-Vese model [9], we use the level set approach to solve the cosegmentation problem given in Eq. (5). In each image, the evolving curve C is represented by the zero level set function $C = \{(x,y) | \phi(x,y) = 0\}$, where the function $\phi: \Omega \to R$ is positive for the points within the region ω and is negative for the points outside ω.

With the Heaviside function $H(\phi)$, which equals with 0 if $\phi < 0$ and with 1 if $\phi \geq 0$, the length of curve C can be expressed as $|C| = \int_{\Omega} |\nabla H(\phi)| \, dxdy$. For the ith counter of image I_k, we have $C_{ki} = \{(x,y) \in \Omega_k : \phi_{ki}(x,y) = 0\}, i \in \{1,2\}$, $\Phi_k = (\phi_{k1}, \phi_{k2})$. Then, the level set formulization of the D-C algorithm can be expressed as follows

$$\begin{aligned} &E_{D-C}^{k}(c_k, \Phi_k) \\ &= \int_{\Omega_k} \left[I_k(x,y) - c_{(1-k)1}\right]^2 H(\phi_{k1}) H(\phi_{k2}) dxdy \\ &+ \int_{\Omega_k} \left[I_k(x,y) - c_{(1-k)2}\right]^2 H(\phi_{k1}) \left(1 - H(\phi_{k2})\right) dxdy \\ &+ \int_{\Omega_k} \left[I_k(x,y) - c_{(1-k)3}\right]^2 \left(1 - H(\phi_{k1})\right) H(\phi_{k2}) dxdy \\ &+ \int_{\Omega_k} \left[I_k(x,y) - c_{(1-k)4}\right]^2 \left(1 - H(\phi_{k1})\right)\left(1 - H(\phi_{k2})\right) dxdy \\ &+ v \sum_{i=1}^{2} \int_{\Omega} |\nabla H(\phi_{ki})| \end{aligned} \quad (6)$$

It should be noted that, different from the classic multiphase level set approach, the energy formulation for each image is computed using the voxel means calculated in the other image. In this way, the information in both the test image or reference image can mutually benefit the counter evolvlution in the other image.

With the associated Euler-Lagrange equations, parameterizing an artificial time t as the descent directions, given the initial curves $\Phi_k(0, x, y)$, and set $\Delta t = 1$, we can use the following rules to perform curve evolution in the image pair. Readers are referred to Ref. [9] for more computational detailes.

$$c_{k1}^{t} = mean(I_k) \; in \; (x,y): \phi_{k1}(t,x,y) > 0, \; \phi_{k2}(t,x,y) > 0\}$$

$$c_{k2}^t = mean(I_k)\ in\ (x,y): \phi_{k1}(t,x,y) > 0,\ \phi_{k2}(t,x,y) < 0\}$$
$$c_{k3}^t = mean(I_k)\ in\ (x,y): \phi_{k1}(t,x,y) < 0,\ \phi_{k2}(t,x,y) > 0\}$$
$$c_{k4}^t = mean(I_k)\ in\ (x,y): \phi_{k1}(t,x,y) < 0,\ \phi_{k2}(t,x,y) < 0\} \quad (7)$$

$$\frac{\partial \phi_{k1}}{\partial t} = \delta_\varepsilon(\phi_{k1})\left\{v\mathrm{div}\left(\frac{\nabla\phi_{k1}}{|\nabla\phi_{k1}|}\right) - \left[\left(\left(I_k - c_{(1-k)1}\right)^2 - \left(I_k - c_{(1-k)3}\right)^2\right)H(\phi_{k2}) + \left(\left(I_k - c_{(1-k)2}\right)^2 - \left(I_k - c_{(1-k)4}\right)^2\right)\left(1 - H(\phi_{k2})\right)\right]\right\}$$
$$\frac{\partial \phi_{k2}}{\partial t} = \delta_\varepsilon(\phi_{k2})\left\{vdiv\left(\frac{\nabla\phi_{k2}}{|\nabla\phi_{k2}|}\right) - \left[\left(\left(I_k - c_{(1-k)1}\right)^2 - \left(I_k - c_{(1-k)2}\right)^2\right)H(\phi_{k1}) + \left(\left(I_k - c_{(1-k)3}\right)^2 - \left(I_k - c_{(1-k)4}\right)^2\right)\left(1 - H(\phi_{k1})\right)\right]\right\} \quad (8)$$

D. Overview

In preprocessing, a reference image for each test brain MR image is generated. Then, each test image and its reference image compose an image pair. With this image pair, the proposed D-C algorithm can be applied to brain segmentation in four steps.

First, we initialize the boundary of each region in the image using the achieved stable segmentation results in the preprocessing step and calculate $\Phi_k(0,x,y)$ and c_k^0 for each image in the image pair. Therefore, the initial counters are defined by the overlapped regions of GM and WM between the atlas and the K-means initialization. Second, the level set function $\Phi_k(t,x,y)$ is updated based on to $\Phi_k(t-1,x,y)$ and c_k^{t-1} according to Eq. (8). Third, the constant vector c_k^t is computed by using Eq. (7). Fourth, the energy of the D-C algorithm can be calculated by using Eq. (6). Then, the second, third and fourth steps are iteratively repeated until the stopping criterion is met. Here, the stopping criteria are either that the optimizing results keep the same for 20 iterations or the total iteration number reaches a limit. Based on our parametric studies, the limit number is set as 300.

The overall segmentation process can be summarized in Algorithm 1.

Algorithm 1: D-C algorithm for image segmentation

Preprocess: construct a reference image using the co-registered atlas and the statistical segmentation results;

For image pairs $I = \{I_k, k = 0,1\}$, simultaneous execute:

1. Initialize: compute $\Phi_k(0,x,y)$ and c_k^0;

For each iteration:

2. Update level set function $\Phi_k(t,x,y)$ corresponding to $\Phi_k(t-1,x,y)$ and c_k^{t-1} using Eq. (8);

3. Update c_k^t with $\Phi_k(t,x,y)$ using Eq. (7);

4. Calculate the energy $E_{D-C}^k(c_k, \Phi_k)$ in Eq. (6)

5. Repeat Steps 2 to 4 until a stopping criterion is met.

III. Experiments and Results

The proposed D-C algorithm has been tested in simulated T1-weighted brain MR images from the BrainWeb [14]. Each image has a dimension of $187 \times 218 \times 187$ and a voxel size of $1 \times 1 \times 1\text{mm}^3$. In our experiments, we used the ICBM452 brain atlas [15]. In each test, we first co-registered the atlas onto the test image by using the statistical parametric mapping (SPM) package [16], and then performed the co-segmentation of the image pair, consisting of the test image and the registered atlas. Since the ground truth for this segmentation task is available, we adopted the following Dice similarity coefficient (DSC) [17] to quantitatively assess the accuracy of the delineation of each brain tissue type. Meanwhile, we calculated the percentage of correctly classified brain voxels to measure the accuracy of the entire brain image segmentation.

Fig. 1(a) shows a T1-weighted brain MR image with 3% noise and 20% intensity non-uniformity (INU). Fig. 1(b) and (c) depict and initial boundaries from brain atlas and the segmentaion result. It reveals that the boundaries are initially blurred and finally became complex enough to match the brain image. The constructed image pair is shown in Fig. 1(d). Compared to the original image, the image pair has avioded numerous kinds of artifacts in the stable segmented voxels, in the manner of which, balanced the comstraint from the atlas and the statistical information. Fig. 1 (e) gives the segmentation results applying multiphase Chan-Vese model based segmentation algorithm [9] to this test image, respectively. Fig. 1(f) shows the ground truth for this segmentation problem. It is clear that the result of the cosegmentation algorithm is much more similar to the ground truth than the result of the other algorithm.

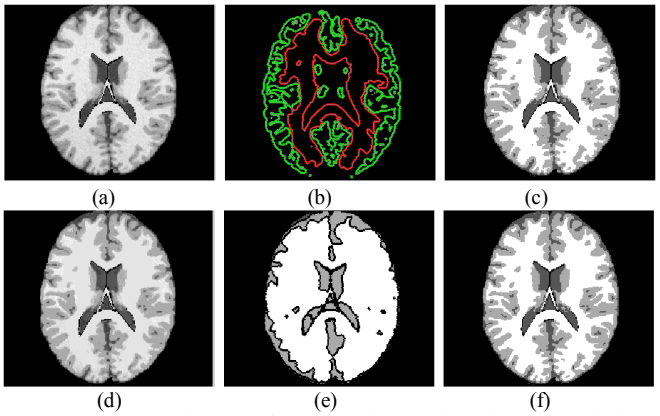

Fig. 1. Comparison between the proposed D-C algorithm and multiphase Chan-Vese model based segmentation algorithm: (a) A T1-weighted brain MR image with 3% noise and 20% INU; (b) Initial boundaries of the proposed algorithm; (c) Segmentation result of the proposed algorithm; (d) Generated image pair; (e) Result of the multiphase Chan-Vese model based algorithm; (f) Ground truth

Next, we compared the D-C algorithm to the state-of-art GA-EM algorithm [6] in a group of T1-weighted brain MR images, which contain 1%, 3%, 5%, and 7% of Gaussian noise with 20% and 40% of INU, respectively. The accuracy of the cosegmentation algorithm in these images was listed in Table 1. The accuracy of both algorithms in segmenting the GM and WM in brain images were compared in Fig.2 and Fig.3. It

shows that the propose algorithm substantially outperforms the GA-EM algorithm in the segmentation of GM and WM.

TABLE I. ACCURACY OF THE PROPOSED SEGMENTATION ALGORITHM IN BRAIN MR IMAGES WITH DIFFERENT LEVELS OF NOISE AND INU

Images	**1% Noise 20% INU**	**3% Noise 20% INU**	**5% Noise 20% INU**	**7% Noise 20% INU**
Accuracy	97.36%	96.36%	94.26%	91.45%
DSC of CSF	97.48%	96.42%	94.82%	92.71%
DSC of GM	96.47%	95.11%	92.33%	88.51%
DSC of WM	98.02%	97.30%	95.58%	93.33%
Images	**1% Noise 40% INU**	**3% Noise 40% INU**	**5% Noise 40% INU**	**7% Noise 40% INU**
Accuracy	95.80%	94.71%	92.70%	89.34%
DSC of CSF	96.78%	95.68%	94.03%	91.75%
DSC of GM	94.41%	92.93%	90.32%	86.05%
DSC of WM	96.60%	95.79%	94.18%	91.26%

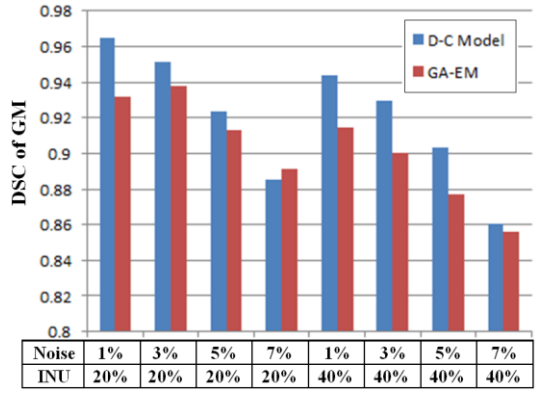

Fig. 2. Comparison of the accuracy of the proposed D-C algorithm and GA-EM algorithm in GM delineation

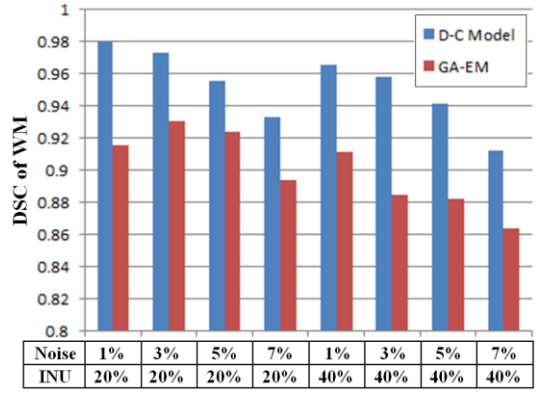

Fig. 3. Comparison of the accuracy of the proposed D-C algorithm and GA-EM algorithm in WM delineation

IV. CONCLUSION

This paper proposes the novel D-C algorithm for brain MR images. Our comparative experiments in T1-weighted MR images with different levels of Gaussian noise and INU demonstrate that the proposed algorithm is capable of solving multiclass image segmentation problems. Moreover, due to the use of an atlas as a reference, the proposed algorithm can achieve robust and much improved segmentation accuracy in highly corrupted brain MR images. In order to futher improve the segmentation performance by addressing the numerous kinds of artifacts, the INU and noise models can be included into the algorithm in the furture.

REFERENCES

[1] P. Aljabar, R. A. Heckemann, A. Hammers, J. V. Hajnal, and D. Rueckert, "Multi-atlas based segmentation of brain images: Atlas selection and its effect on accuracy," *NeuroImage,* vol. 46, pp. 726-738, 2009.

[2] B. Fischl, D. H. Salat, E. Busa, M. Albert, M. Dieterich, C. Haselgrove, A. van der Kouwe, R. Killiany, D. Kennedy, S. Klaveness, A. Montillo, N. Makris, B. Rosen, and A. M. Dale, "Whole Brain Segmentation: Automated Labeling of Neuroanatomical Structures in the Human Brain," Neuron, vol. 33, pp. 341-355, 2002.

[3] R. A. Heckemann, J. V. Hajnal, P. Aljabar, D. Rueckert, and A. Hammers, "Automatic anatomical brain MRI segmentation combining label propagation and decision fusion," NeuroImage, vol. 33, pp. 115-126, 2006.

[4] T. Zhang, Y. Xia, and D. D. Feng, "Clonal selection algorithm for Gaussian mixture model based segmentation of 3D brain MR Images," presented at the IscIDE2011.

[5] G. Tian, Y. Xia, Y. Zhang, and D. Feng, "Hybrid Genetic and Variational Expectation-Maximization Algorithm for Gaussian-Mixture-Model-Based Brain MR Image Segmentation," Information Technology in Biomedicine, IEEE Transactions on, vol. 15, pp. 373-380, 2011.

[6] J. Tohka, E. Krestyannikov, I. D. Dinov, A. M. Graham, D. W. Shattuck, U. Ruotsalainen, and A. W. Toga, "Genetic Algorithms for Finite Mixture Model Based Voxel Classification in Neuroimaging," Medical Imaging, IEEE Transactions on, vol. 26, pp. 696-711, 2007.

[7] D. Mumford and J. Shah, "Optimal approximations by piecewise smooth functions and associated variational problems," Communications on Pure and Applied Mathematics, vol. 42, pp. 577-685, 1989.

[8] T. F. Chan and L. A. Vese, "Active contours without edges," Image Processing, IEEE Transactions on, vol. 10, pp. 266-277, 2001.

[9] L. A. Vese and T. F. Chan, "A Multiphase Level Set Framework for Image Segmentation Using the Mumford and Shah Model," International Journal of Computer Vision, vol. 50, pp. 271-293, 2002.

[10] S. Vicente, V. Kolmogorov, and C. Rother, "Cosegmentation Revisited: Models and Optimization Computer Vision – ECCV 2010." vol. 6312, K. Daniilidis, P. Maragos, and N. Paragios, Eds., ed: Springer Berlin / Heidelberg, 2010, pp. 465-479.

[11] S. Vicente, C. Rother, and V. Kolmogorov, "Object cosegmentation," in Computer Vision and Pattern Recognition (CVPR), 2011 IEEE Conference on, 2011, pp. 2217-2224.

[12] D. Batra, A. Kowdle, D. Parikh, L. Jiebo, and C. Tsuhan, "iCoseg: Interactive co-segmentation with intelligent scribble guidance," in Computer Vision and Pattern Recognition (CVPR), 2010 IEEE Conference on, 2010, pp. 3169-3176.

[13] F. Meng, H. Li, and G. Liu, "Image Co-Segmentation via Active Contours," presented at the ISCAS 2012, COEX, Seoul, Korea.

[14] C. A. Cocosco, V. Kollokian, R. K.-S. Kwan, and A. C. Evans, "BrainWeb: Online Interface to a 3D MRI Simulated Brain Database," *NeuroImage,* vol. 5, 1997.

[15] J. C. Mazziotta and A. W. Toga. International Consortium for Brain Mapping [Online]. Available: http://www.loni.ucla.edu/ICBM/ICBM TissueProb.html

[16] (2009). Statistical Parameter Mapping. Available: http://www.fil.ion.ucl.ac.uk/spm/software/spm8/

[17] A. Bharatha, M. Hirose, N. Hata, S. K. Warfield, M. Ferrant, K. H. Zou, E. Suarez-Santana, J. Ruiz-Alzola, A. D. Amico, R. A. Cormack, R. Kikinis, F. A. Jolesz, and C. M. Tempany, "Evaluation of three-dimensional finite element-based deformable registration of pre- and intra-operative prostate imaging," *Medical Physics,* vol. 28, 2001.